Analytical application of the recursion and moments methods to the electronic structure of C_{60}: Exact solution for the π and σ states

Yeong-Lieh Lin* and Franco Nori
Department of Physics, The University of Michigan, Ann Arbor, Michigan 48109-1120
(Received 28 August 1995)

The recursion and moments methods are applied analytically to study the electronic structure of a neutral C_{60} molecule. We employ a tight-binding Hamiltonian which considers both the *s and p* valence electrons of carbon. From the recursion method, we obtain *exact* results for the π *and* σ eigenvalues and eigenfunctions, including the highest occupied molecular orbital and the lowest unoccupied molecular orbital states. We also compute the Green's function in analytic closed form and obtain the local density of states around several *ring clusters*, which can be probed experimentally by using, for instance, a scanning tunneling microscope. From the method of moments, identical results for the energy spectrum are also derived. In addition, the local density of states on *one* carbon atom is obtained; from this we can derive the degree of degeneracy of the energy levels.

I. INTRODUCTION AND SUMMARY OF RESULTS

Since the discovery of a simple technique for the production in bulk quantities of fullerenes, undoped and doped C_{60} molecules have generated enormous interest among chemists, physicists, and materials scientists. In C_{60}, carbon atoms sit at the 60 vertices of the pentagons and hexagons of a truncated icosahedron. The carbon-carbon bonds are of two different lengths: 1.46 Å for the single bonds (bonds on the pentagons) and 1.40 Å for the double bonds (bonds on the hexagons not shared by a pentagon). The single (double) bonds are denoted by solid (dotted) lines throughout the figures in this paper. The literature on C_{60} is vast, and here we do not attempt a review. The interested reader is referred to Refs. 1–7 and papers listed therein.

In this work, we focus on an *analytical* study of the electronic structure of a single neutral C_{60} molecule. We model this system through a tight-binding Hamiltonian [Eq. (1)] which considers both the *s* and *p* valence electrons of carbon. For decades, the recursion method and method of moments have been successfully applied to the electronic structure calculations in a variety of physical systems. However, most of these applications have been purely numerical. Furthermore, the relationship between these two methods has rarely been investigated thoroughly. The goal of this paper is to *analytically* apply these two methods to study the electronic structure of a C_{60} molecule. Relations between these two approaches will be discussed.

This paper is organized as follows. In Sec. II, we discuss the physical nature and types of the interaction between these valence electrons, with a total number of 240. The couplings can be separated into two main contributions: coming from the π-bonded and σ-bonded electrons.

We first focus on the π states. In Sec. III we use the recursion method[8] to analytically solve the Hamiltonian for the π electrons. We derive *closed-form expressions* for their energy eigenvalues and eigenfunctions—including the highest occupied molecular orbital (HOMO) and the lowest unoccupied molecular orbital (LUMO)—for two cases: equal and unequal hopping integrals for the single and double bonds. The main results concerning the π-state eigenvalues and eigenfunctions are summarized in Tables III, IV, and V. The physical nature of the wave functions of the HOMO and LUMO is discussed in Sec. III D. The beauty of the recursion method for C_{60} lies in the fact that the recurrence is simple and terminates very quickly (e.g., after *four* iterations only), providing exact and very concise expressions for the parameters of the recursion. Thus, the dimensionality of the problem is reduced by a factor of 15, namely from 60×60 to 4×4.

The same results for the energy spectrum of the π states are derived in Sec. IV by using the method of moments. The main ingredient in this approach is the analytical computation of sums over contributions from *all* paths starting and ending at the same site, each one with its corresponding kinetic energy. The spirit of this approach follows Feynman's program: to compute physical quantities from sums over paths. In addition, the local density of states (LDOS) on one carbon atom is obtained; from this we can derive the degree of degeneracy of the energy levels.

In the two sections mentioned above, we provide detailed descriptions of the steps (e.g., the choice of appropriate starting states incorporating the physical properties of the system, and the iteration schemes) employed in the analytic application of the recursion and moments methods to C_{60}. Furthermore, every step of either approach is exact. All the calculations are done analytically, either by hand or with the assistance of computer symbolic manipulation software. Diagonalizations are achieved by iteratively applying the Hamiltonian on simple initial states.

The relations between the recursion and moments methods are discussed in Sec. V. There it will be seen that while these two approaches are related to each other, each one has its own advantages. These methods are significantly different from the ones used so far. Furthermore, they are *neither* numerical *nor* require the use of group theory. For a lucid and clear account of a very different approach, based on group theory and focused only on the π states, the reader is referred to Ref. 3.

In Sec. VI, we present the precise algebraic expressions, derived from the Green's functions, as well as plots of the LDOS around several ring clusters (i.e., a carbon atom, a

pentagon ring, and a hexagon ring; also for two opposite carbon atoms, pentagons, and hexagons). We find that around a pentagon ring the LDOS is large at low energies. This is related to the fact that a pentagon has zero double bonds and five single bonds. On the other hand, around a hexagon ring the LDOS is large at high energies. This is because a hexagon has three double bonds and three single bonds. The LDOS is relevant to the several important experimental techniques which probe the *local* spectroscopy of molecules; for instance, by using a scanning tunneling microscope, as described in the review in Ref. 9.

In Sec. VII we discuss the solutions of the σ-states Hamiltonian Eq. (3). To describe the σ states, the coupling between orbitals on the same atom and that between orbitals along the same bond are both taken into account. By following a ''one band—two band'' transformation,[10] the eigenvalues and eigenfunctions for the σ states are then analytically obtained.

II. ELECTRONIC STATES

To investigate the electronic properties of a single C_{60} molecule, we consider the four carbon valence electrons $2s$, $2p_x$, $2p_y$, and $2p_z$ in the tight-binding Hamiltonian

$$\mathbf{H}_T=\sum_{i,\alpha}\epsilon_\alpha c_{i\alpha}^\dagger c_{i\alpha}+\sum_{\langle ij\rangle,\alpha,\beta}t_{\alpha\beta}c_{i\alpha}^\dagger c_{j\beta}. \tag{1}$$

Here, i denotes the carbon site and α denotes the valence orbitals $2s$, $2p_x$, $2p_y$, and $2p_z$. Also, ϵ_α is the orbital energy and $t_{\alpha\beta}$ is the hopping matrix element between orbitals on the nearest-neighboring sites i and j. The 60 $2p_z$ orbitals, each pointing along the outward radial direction, are hybridized to form π states. The other three orbitals $2s$, $2p_x$, and $2p_y$, distributed on the plane tangential to the surface of the molecule, are hybridized along the lattice bonds to form σ bonding and antibonding states.

Let us assume that the mixture of these three orbitals at each site produces three sp^2 hybrid orbitals: sp_a^2 along the double bond and sp_b^2 and sp_c^2 along the two single bonds, respectively. From a physical point of view, the 60 outer π orbitals are relevant to the conducting properties of the molecules and the 180 σ orbitals are mainly responsible for the elastic properties. The former are also responsible for the bond dimerization. Also, only π states occur around the Fermi energy.

As a result of its planar structure, the π electrons in graphite contain only pure $2p_z$ orbitals. Nevertheless, in the curved structure of C_{60}, an extra small component from $2s$, $2p_x$, and $2p_y$ is induced along the radial direction due to the surface curvature. The interaction between the π orbitals in C_{60} is then slightly increased in comparison to that in graphite. However, since this component is very small, the overlap integral between π and σ orbitals is negligible. The nonzero Hamiltonian parameters used here are the same ones as in Ref. 2.

The original Hamiltonian Eq. (1) can thus be written in terms of $\mathbf{H}_\pi$ and $\mathbf{H}_\sigma$ as $\mathbf{H}_T=\mathbf{H}_\pi\oplus\mathbf{H}_\sigma$, where

$$\mathbf{H}_\pi=-\sum_{\langle ij\rangle}t_{ij}c_i^\dagger c_j \tag{2}$$

and

$$\mathbf{H}_\sigma=-V_1\sum_{i,\alpha\neq\beta}c_{i\alpha}^\dagger c_{i\beta}-V_2\sum_{\langle ij\rangle}c_{i\alpha}^\dagger c_{j\alpha}. \tag{3}$$

The electronic π-states Hamiltonian Eq. (2) describes the kinetic energy of the $2p_z$ electrons hopping on the 60 vertices of a C_{60} fullerene and t_{ij} is the hopping integral between nearest-neighboring atoms i and j. The hopping integrals are considered unequal for single and double bonds. Also $c_i^\dagger$ is the electron operator creating a $2p_z$ orbital on the atom located at vertex i. A constant term corresponding to the on-site $2p_z$ orbital energy is omitted in Eq. (2). In the σ-states Hamiltonian Eq. (3), $\alpha=sp_a^2$, sp_b^2, and sp_c^2 denotes the hybridized orbitals. Also, V_1 stands for the hopping integral between orbitals on the same carbon atom and V_2 stands for that between orbitals on different atoms that are associated with the same bond (the length difference between single and double bonds is neglected here). A more detailed discussion on the origin of V_1 and V_2 is presented in Appendix A.

Admittedly, this is a simplified model (like the ''Ising model'') for the electronic structure of C_{60}, the ''hydrogen atom'' of the main fullerene family of C_{60n^2} molecules. However, its understanding is a convenient stepping stone to the study of more complex models. The spectroscopy of, for instance, the hydrogen atom can be analytically solved by using several different approaches. These lead to the same analytical expressions for the eigenvalues and eigenvectors. In spite of the fact that modern computers can easily obtain numerical expressions for them, it is useful to have analytic results. In fact, analytical solutions have always been pursued in the area of spectroscopy of atoms, molecules, and clusters. In this paper, we pursue several approaches to the analytical study of the spectroscopy of an important molecule. We would like to emphasize that the approaches described here are not intended to substitute more traditional methods, but to present alternative viewpoints and complementary results.

III. RECURSION METHOD APPROACH

A. Formulation

We first focus on the π-states Hamiltonian Eq. (2). Let us begin with a brief outline of the recursion method[8] for obtaining the eigenvalues and eigenfunctions. First, one must choose an appropriate normalized starting state $|f_0\rangle$. Further states are iteratively generated by the three-term recurrence relation

$$\mathbf{H}|f_n\rangle=a_n|f_n\rangle+b_{n+1}|f_{n+1}\rangle+b_n|f_{n-1}\rangle, \tag{4}$$

with the condition $b_0|f_{-1}\rangle\equiv 0$. Here, the real parameters a_n and b_{n+1} are determined by

$$a_n=\langle f_n|\mathbf{H}|f_n\rangle \tag{5}$$

and

$$b_{n+1}=\langle f_n|\mathbf{H}|f_{n+1}\rangle=\langle f_{n+1}|\mathbf{H}|f_n\rangle. \tag{6}$$

By convention, the b's are chosen to be positive. The process terminates at $|f_{N-1}\rangle$ with the last recurrence $\mathbf{H}|f_{N-1}\rangle=a_{N-1}|f_{N-1}\rangle+b_{N-1}|f_{N-2}\rangle$. The constructed orthonormal

states $\{|f_0\rangle,|f_1\rangle,\ldots,|f_{N-1}\rangle\}$ along with the parameters $\{a_0,a_1,\ldots,a_{N-1}\}$ and $\{b_1,b_2,\ldots,b_{N-1}\}$ thus constitute the "chain model"[8] of a given Hamiltonian. The representation of $\mathbf{H}$ in the new basis $\{|f_n\rangle\}$ is in a tridiagonal form.

The energy levels can be achieved by constructing the following polynomials with $P_{-1}(E)=0$ and $P_0(E)=1$:

$$P_{n+1}(E)=\frac{(E-a_n)P_n(E)-b_nP_{n-1}(E)}{b_{n+1}}. \tag{7}$$

The eigenvalues E_λ are determined by the N zeros of the last polynomial $P_N(E)=0$, with an arbitrary nonzero b_N. It follows then that the eigenfunctions are

$$\frac{1}{\mathcal{N}_\lambda}\sum_{n=0}^{N-1}P_n(E_\lambda)|f_n\rangle, \tag{8}$$

where $\mathcal{N}_\lambda=[\Sigma_{n=0}^{N-1}P_n^2(E_\lambda)]^{1/2}$ are the normalization constants for the eigenfunctions, and $P_0(E_\lambda)$ always equals 1.

So far, we have briefly outlined the recursion method. We now come to the application of this approach to the electronic structure of a fullerene molecule. For convenience, we work in units of the single-bond hopping integral. The hopping amplitude is therefore 1 for every single bond and t for each double bond. It has been pointed out[1] that the value of t is about 1.1. We will use two alternative sets (denoted by $\mathcal{A}$ and $\mathcal{B}$) of starting states. Each set consists of two initial states from which the whole energy spectrum can be derived, and the final results do not depend on the choice of initial bases. Both sets lead to the *same* solutions for the eigenvalues and eigenfunctions. From the physical point of view, this consistency ensures the equivalent interpretation of the results from these two sets of initial states. We denote by $|j\rangle$ the $2p_z$ orbital centered at the jth atom. For convenience of visualization, in all our figures we flatten the truncated icosahedral structure of C_{60} into a plane. Note that labelings vary according to the different choices of initial states.

B. Case $\mathcal{A}$

The first set of initial states starts from a five-atom pentagon ring [see Fig. 1(a)] and a six-atom hexagon ring [see Fig. 1(b)]. Starting from a pentagon ring, we choose the initial state $|u_0\rangle$ as a linear combination of the five orbitals on it,

$$|u_0\rangle=\frac{1}{\sqrt{5}}\sum_{j=1}^{5}|j\rangle. \tag{9}$$

Here the labeling is as shown in Fig. 1(a). From now on, $\mathbf{H}$ will denote $\mathbf{H}_\pi$ unless specified otherwise (e.g., $\mathbf{H}_\sigma$). As an illustration, we present here the calculation of the first recurrence,

$$\begin{aligned}\mathbf{H}|u_0\rangle=&-\frac{1}{\sqrt{5}}[(|2\rangle+|5\rangle+t|6\rangle)+(|1\rangle+|3\rangle+t|7\rangle)+(|2\rangle\\&+|4\rangle+t|8\rangle)+(|3\rangle+|5\rangle+t|9\rangle)+(|1\rangle+|4\rangle\\&+t|10\rangle)]\\=&-2\left[\frac{1}{\sqrt{5}}(|1\rangle+|2\rangle+|3\rangle+|4\rangle+|5\rangle)\right]\\&+t\left[-\frac{1}{\sqrt{5}}(|6\rangle+|7\rangle+|8\rangle+|9\rangle+|10\rangle)\right]\\=&-2|u_0\rangle+t|u_1\rangle.\end{aligned}$$

We then obtain $a_0=-2$, $b_1=t$, and $|u_1\rangle=-1/\sqrt{5}\,\Sigma_{j=6}^{10}|j\rangle$. Following the same procedure, we can construct further states and obtain the parameters a's and b's at the same time. The beauty of the recursion method for C_{60} lies in the fact that the recurrence terminates very quickly, exactly at $|u_7\rangle$. As a result, we have exact and very concise formulas for a_0 through a_7, and b_1 through b_7.

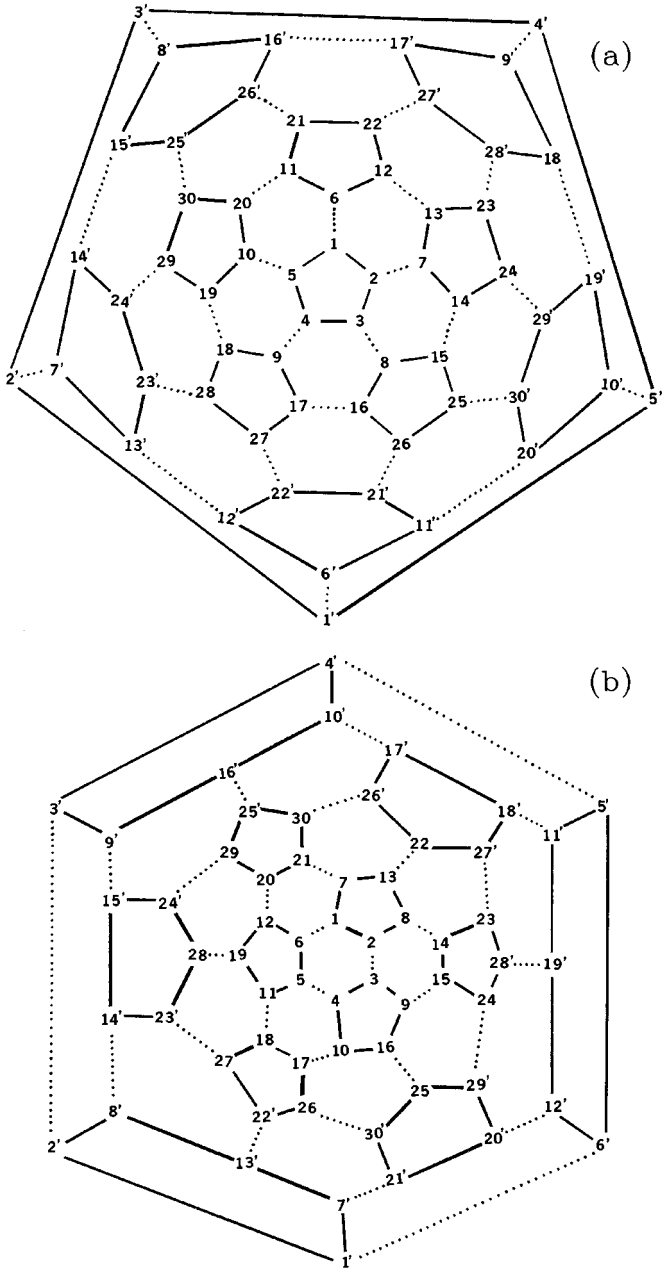

FIG. 1. Flattened C_{60} molecule obtained by stretching (a) a pentagon and (b) a hexagon, with the site labels used in cases $\mathcal{A}$ and $\mathcal{B}$ in the recursion method.

TABLE I. States and parameters for case $\mathscr{A}$ in the recursion method approach. It is interesting to notice that $a_n = a_{7-n}$ and $b_n = b_{8-n}$ for $n = 4,5,6,7$.

n	Starting from a pentagon ring $\lvert u_n\rangle$	a_n	b_n	Starting from a hexagon ring $\lvert v_n\rangle$	a_n	b_n
0	$\frac{1}{\sqrt{5}}\Sigma_{j=1}^{5}\lvert j\rangle$	-2		$\frac{1}{\sqrt{6}}\Sigma_{j=1}^{6}(-1)^{j+1}\lvert j\rangle$	$1+t$	
1	$-\frac{1}{\sqrt{5}}\Sigma_{j=6}^{10}\lvert j\rangle$	0	t	$\frac{1}{\sqrt{6}}\Sigma_{j=7}^{12}(-1)^{j}\lvert j\rangle$	0	1
2	$\frac{1}{\sqrt{10}}\Sigma_{j=11}^{20}\lvert j\rangle$	$-t$	$\sqrt{2}$	$\frac{1}{\sqrt{6}}\Sigma_{j=14}^{15}(-1)^{j+1}[\lvert j\rangle+\lvert j+3\rangle+\lvert j+6\rangle]$	1	t
3	$-\frac{1}{\sqrt{10}}\Sigma_{j=21}^{30}\lvert j\rangle$	-1	1	$\frac{1}{\sqrt{6}}\Sigma_{j=23}^{24}(-1)^{j+1}[\lvert j\rangle+\lvert j+3\rangle+\lvert j+6\rangle]$	0	1
4	$\frac{1}{\sqrt{10}}\Sigma_{j=21}^{30}\lvert j'\rangle$	-1	t	$\frac{1}{\sqrt{6}}\Sigma_{j=23}^{24}(-1)^{j+1}[\lvert j'\rangle+\lvert (j+3)'\rangle+\lvert (j+6)'\rangle]$	0	t
5	$-\frac{1}{\sqrt{10}}\Sigma_{j=11}^{20}\lvert j'\rangle$	$-t$	1	$\frac{1}{\sqrt{6}}\Sigma_{j=14}^{15}(-1)^{j+1}[\lvert j'\rangle+\lvert (j+3)'\rangle+\lvert (j+6)'\rangle]$	1	1
6	$\frac{1}{\sqrt{5}}\Sigma_{j=6}^{10}\lvert j'\rangle$	0	$\sqrt{2}$	$\frac{1}{\sqrt{6}}\Sigma_{j=7}^{12}(-1)^{j}\lvert j'\rangle$	0	t
7	$-\frac{1}{\sqrt{5}}\Sigma_{j=1}^{5}\lvert j'\rangle$	-2	t	$\frac{1}{\sqrt{6}}\Sigma_{j=1}^{6}(-1)^{j+1}\lvert j'\rangle$	$1+t$	1

Similarly, starting from a linear combination of the six orbitals on a hexagon ring, we have the initial state $\lvert v_0\rangle$ as

$$\lvert v_0\rangle = \frac{1}{\sqrt{6}}\sum_{j=1}^{6}(-1)^{j+1}\lvert j\rangle, \tag{10}$$

where the labeling is referred to Fig. 1(b). The choice of alternating signs, $(-1)^{j+1}$, meets the threefold symmetry requirement of a hexagon ring in C_{60}, with alternating single and double bonds. Again, the recurrence terminates at $\lvert v_7\rangle$. We then obtain another group of parameters a's and b's. All these $\lvert u_n\rangle$ and $\lvert v_n\rangle$ states, as well as their respective parameters a_n and b_{n+1}, are summarized in Table I.

Through these two groups of a's and b's, we can, respectively, construct two polynomials $P_8^p(E)$ and $P_8^h(E)$ which are of eighth degree in E. Here the superscript p for pentagon (h for hexagon) refers to the polynomial constructed from the group of a's and b's generated by $\lvert u_0\rangle$ ($\lvert v_0\rangle$). The roots of these two polynomials can be analytically obtained and correspond to the electronic energy levels. It follows then that we have a total of 16 distinct eigenvalues. When $t=1$, a common root -1 exists for both polynomials P_8^p and P_8^h. We thus have 15 distinct energy levels. It is also straightforward to obtain the eigenvectors through Eq. (8).

C. Case $\mathscr{B}$

In this approach, we exploit the symmetry property that the inversion operator leaves the C_{60} molecule invariant. We therefore take the first (second) starting state $\lvert\phi_0\rangle$ ($\lvert\varphi_0\rangle$) as a linear combination of the orbitals on two opposite (i.e., antipodes) pentagon (hexagon) rings

$$\lvert\phi_0\rangle = \frac{1}{\sqrt{10}}\sum_{j=1}^{5}(\lvert j\rangle+\mathscr{P}\lvert j'\rangle) \tag{11}$$

and

$$\lvert\varphi_0\rangle = \frac{1}{\sqrt{12}}\sum_{j=1}^{6}(-1)^{j+1}(\lvert j\rangle+\mathscr{P}\lvert j'\rangle), \tag{12}$$

where the site labels are presented in Fig. 1(a) [1(b)] for the first (second) starting state. Here $\mathscr{P}$ stands for parity, with the value $+1$ or -1. Note that atom j and atom j' are antipodes. Following the same procedure, we find the very convenient and remarkable result that *the recurrence terminates even faster* at $\lvert\phi_3\rangle$ ($\lvert\varphi_3\rangle$) for the first (second) initial state. Due to the two possible values of $\mathscr{P}$, we have two different results for a_3 for each starting state. In Appendix B we present the calculation of the last recurrence, namely those for $\lvert\phi_3\rangle$ and $\lvert\varphi_3\rangle$. It can be clearly seen that $\mathbf{H}\lvert\phi_3\rangle$ generates two possible values for a_3 and no further state; and so does $\mathbf{H}\lvert\varphi_3\rangle$. As a consequence, we obtain four groups of $\{a_0,a_1,a_2,a_3\}$ and $\{b_1,b_2,b_3\}$.

All the states $\lvert\phi_n\rangle$ and $\lvert\varphi_n\rangle$, as well as their respective parameters a_n and b_{n+1}, are listed in Table II. It follows that we can construct four polynomials $P_4^{p+}(E)$, $P_4^{p-}(E)$, $P_4^{h+}(E)$, and $P_4^{h-}(E)$. Each one is of fourth degree in E. The superscript $p+$ stands for the polynomial constructed from $\lvert\phi_0\rangle$ with $\mathscr{P}$ equal to $+1$, and similarly for the others. With the choice of $b_4 = 1/b_1b_2b_3$, these polynomials can be explicitly written as

$$P_4^{p+}(E) = E^4+(2t+3)E^3+(5t-1)E^2-(2t^3-t^2+8)E -(t+2)(t^3-t^2+t+2),$$

$$P_4^{p-}(E) = E^4+3E^3-(2t^2-t+1)E^2-(3t^2-4t+8)E +(t^4-t^3+t^2+4t-4),$$

$$P_4^{h+}(E) = E^4-2(t+1)E^3+(3t-1)E^2-(2t^3+t+2)E -(t^2+1)(t^2+t-1),$$

and

TABLE II. States and parameters for case $\mathscr{B}$ in the recursion method approach. The parity $\mathscr{P}$ can be $+1$ or -1.

n	Starting from two opposite pentagon rings $\lvert\phi_n\rangle$	a_n	b_n
0	$\frac{1}{\sqrt{10}}\Sigma_{j=1}^{5}[\lvert j\rangle+\mathscr{P}\lvert j'\rangle]$	-2	
1	$-\frac{1}{\sqrt{10}}\Sigma_{j=6}^{10}[\lvert j\rangle+\mathscr{P}\lvert j'\rangle]$	0	t
2	$\frac{1}{\sqrt{20}}\Sigma_{j=11}^{20}[\lvert j\rangle+\mathscr{P}\lvert j'\rangle]$	$-t$	$\sqrt{2}$
3	$-\frac{1}{\sqrt{20}}\Sigma_{j=21}^{30}[\lvert j\rangle+\mathscr{P}\lvert j'\rangle]$	$-(1+\mathscr{P}t)$	1
n	Starting from two opposite hexagon rings $\lvert\varphi_n\rangle$	a_n	b_n
0	$\frac{1}{\sqrt{12}}\Sigma_{j=1}^{6}(-1)^{j+1}[\lvert j\rangle+\mathscr{P}\lvert j'\rangle]$	$1+t$	
1	$\frac{1}{\sqrt{12}}\Sigma_{j=7}^{12}(-1)^{j}[\lvert j\rangle+\mathscr{P}\lvert j'\rangle]$	0	1
2	$\frac{1}{\sqrt{12}}\Sigma_{j=14}^{15}(-1)^{j+1}[\lvert j\rangle+\lvert j+3\rangle+\lvert j+6\rangle+\mathscr{P}(\lvert j'\rangle+\lvert(j+3)'\rangle+\lvert(j+6)'\rangle)]$	1	t
3	$\frac{1}{\sqrt{12}}\Sigma_{j=23}^{24}(-1)^{j+1}[\lvert j\rangle+\lvert j+3\rangle+\lvert j+6\rangle+\mathscr{P}(\lvert j'\rangle+\lvert(j+3)'\rangle+\lvert(j+6)'\rangle)]$	$\mathscr{P}t$	1

$$P_4^{h-}(E)=E^4-2E^3-(2t^2+t+1)E^2-(2t^2+t+2)E-(t+1)^2(t^2-t+1).$$

By analytically solving these four polynomials, we obtain the same 16 eigenvalues obtained above (case $\mathscr{A}$). Similarly we can obtain the eigenvectors, which are also equal to those obtained from the alternative set $\mathscr{A}$ of initial states.

D. Results for the π-state eigenvalues and eigenfunctions of C_{60}

In Table III, we summarize the eigenvalues and the corresponding eigenvectors for the case $t=1$. In Table IV, we present the closed-form eigenvalues—including the HOMO and LUMO energies—explicitly expressed in terms of the single-bond hopping integral t_1 and the double-bond hopping integral t_2. Thus, eigenvalues for the limiting cases $t_1=0$ or $t_2=0$ can also be readily inferred.

It is interesting to note that the fivefold degenerate HOMO state is obtained from the initial state $\lvert\varphi_0\rangle$ (with negative parity), made of orbitals on two opposite hexagons with a threefold symmetry axis passing through their centers. On the other hand, the threefold degenerate LUMO state is obtained from the initial state $\lvert\phi_0\rangle$ (with negative parity), consisting of orbitals on two opposite pentagons with a fivefold symmetry axis passing through their centers.

As to the eigenfunctions, we present in Table V those for the HOMO and LUMO in terms of $t=t_1/t_2$, the ratio of the hopping matrix elements for single and double bonds. Since the respective degree of degeneracy for each eigenvalue can be acquired from the local density of states on a carbon atom (discussed in a later section), the other degenerate eigenvectors can be generated by standard group theory analysis. This is outside the scope of the present paper. We therefore only present these eigenfunctions derived from the pure application of the recursion method.

It is instructive to notice that the following points further support the results for the degeneracy. They are (1) the sum of the product of energy and its corresponding degeneracy equals the trace of the Hamiltonian, which is zero; (2) the number of states with even parity equals that with odd parity; and (3) the behavior of the eigenvalues can be easily studied in the limits when either $t_1=0$ or $t_2=0$.

E. Relations between alternatives $\mathscr{A}$ and $\mathscr{B}$

It is worthwhile to point out the following relations between the cases $\mathscr{A}$ and $\mathscr{B}$ presented before. First, $P_8^p(E)=P_4^{p+}(E)P_4^{p-}(E)$ and $P_8^h(E)=P_4^{h+}(E)P_4^{h-}(E)$ up to an overall constant factor. In other words, roots solved from $P_8^p(E)$ $[P_8^h(E)]$ are identical to those solved from $P_4^{p+}(E)$ and $P_4^{p-}(E)$ $[P_4^{h+}(E)$ and $P_4^{h-}(E)]$. Second, from Tables I and II we can see that, for $n=0$, 1, 2 and 3,

$$\lvert\phi_n\rangle=\frac{1}{\sqrt{2}}(\lvert u_n\rangle-\mathscr{P}\lvert u_{7-n}\rangle)$$

and

$$|\varphi_n\rangle=\frac{1}{\sqrt{2}}(|v_n\rangle+\mathscr{P}|v_{7-n}\rangle).$$

Third, for those eigenvalues E_λ which are common roots of P_8^p and P_4^{p+}, or common roots of P_8^h and P_4^{h-},

$$P_{7-n}(E_\lambda)=-P_n(E_\lambda).$$

Also for those eigenvalues E_λ which are common roots of P_8^p and P_4^{p-}, or common roots of P_8^h and P_4^{h+},

$$P_{7-n}(E_\lambda)=P_n(E_\lambda).$$

Here, all the $P_n(E_\lambda)$'s refer to the polynomials constructed in the case $\mathscr{A}$ and $n=0,1,2,$ and 3. Fourth, $P_1(E_\lambda)$, $P_2(E_\lambda)$, and $P_3(E_\lambda)$ calculated from the two alternatives $\mathscr{A}$ and $\mathscr{B}$ are the same. Fifth, for the eigenvector with respect to the same eigenvalue, the normalization constants $\mathscr{N}_\mathscr{A}$ and $\mathscr{N}_\mathscr{B}$, calculated in $\mathscr{A}$ and $\mathscr{B}$, respectively, satisfy $\mathscr{N}_\mathscr{A}=\sqrt{2}\mathscr{N}_\mathscr{B}$.

From the above five properties, the equivalence of results from both alternatives becomes clear. As an example, for an eigenvalue E_λ which is a common root of P_8^p and P_4^{p+}, we can obtain the eigenvector $|\Psi_\lambda\rangle$ from $\mathscr{A}$ as

$$\begin{aligned}|\Psi_\lambda\rangle&=\frac{1}{\mathscr{N}_\mathscr{A}}\sum_{n=0}^{7}P_n(E_\lambda)|u_n\rangle\\&=\frac{\sqrt{2}}{\mathscr{N}_\mathscr{A}}\left[P_0\frac{1}{\sqrt{2}}(|u_0\rangle-|u_7\rangle)+P_1\frac{1}{\sqrt{2}}(|u_1\rangle-|u_6\rangle)\right.\\&\quad\left.+P_2\frac{1}{\sqrt{2}}(|u_2\rangle-|u_5\rangle)+P_3\frac{1}{\sqrt{2}}(|u_3\rangle-|u_4\rangle)\right]\\&=\frac{1}{\mathscr{N}_\mathscr{B}}\sum_{n=0}^{3}P_n(E_\lambda)|\phi_n\rangle,\end{aligned}$$

where the last equality is just the result obtained directly from $\mathscr{B}$. In fact, from the results of alternative $\mathscr{A}$, we can understand the parity property associated with C_{60}.

IV. METHOD OF MOMENTS APPROACH

A. Methodology and application

In this method, the first and central task is the computation of moments, defined by

$$\mathscr{M}_l\equiv\langle j|\mathbf{H}^l|j\rangle, \tag{13}$$

where the order l is a positive integer. Note that $\mathscr{M}_0=1$ when $l=0$. The physical meaning of the above quantum-mechanical expectation value is as follows. The Hamiltonian

TABLE III. The eigenvalues E_λ and the corresponding eigenvectors $(1/\mathscr{N}_\lambda)\,\Sigma_{n=0}^{3}P_n(E_\lambda)|f_n\rangle$ for C_{60} with $t=1$. Recall that $P_0(E_\lambda)$ is always equal to 1. Here $|\phi_n^\pm\rangle$ ($|\varphi_n^\pm\rangle$) denotes $|\phi_n\rangle$ ($|\varphi_n\rangle$) with $\mathscr{P}=\pm1$. Also $\alpha=\sqrt{2(19+\sqrt{5})}$ and $\beta=\sqrt{2(19-\sqrt{5})}$. Notice that the HOMO energy is $(1-\sqrt{5})/2$ and the LUMO energy is $(-3-\sqrt{5}+\beta)/4$.

E_λ	$P_1(E_\lambda)$	$P_2(E_\lambda)$	$P_3(E_\lambda)$	$\mathscr{N}_\lambda^2$	$\lvert f_n\rangle$
-3	-1	$\sqrt{2}$	$-\sqrt{2}$	6	$\lvert\phi_n^+\rangle$
-1	1	$-\sqrt{2}$	$-\sqrt{2}$	6	$\lvert\phi_n^+\rangle$
$(-1+\sqrt{13})/2\simeq1.303$	$(3+\sqrt{13})/2$	$\sqrt{2}(3+\sqrt{13})/4$	$\sqrt{2}/2$	$(39+9\sqrt{13})/4$	$\lvert\phi_n^+\rangle$
$(-1-\sqrt{13})/2\simeq-2.303$	$(3-\sqrt{13})/2$	$\sqrt{2}(3-\sqrt{13})/4$	$\sqrt{2}/2$	$(39-9\sqrt{13})/4$	$\lvert\phi_n^+\rangle$
$(-3+\sqrt{5}+\alpha)/4\simeq1.438$	$\frac{5+\sqrt{5}+\alpha}{4}$	$\frac{\sqrt{2}[6+2\sqrt{5}+(\sqrt{5}+1)\alpha]}{16}$	$\frac{\sqrt{2}[-4+8\sqrt{5}+(\sqrt{5}-1)\alpha]}{16}$	$\frac{95+5\sqrt{5}}{8}+\frac{(25+\sqrt{5})\alpha}{16}$	$\lvert\phi_n^-\rangle$
$(-3+\sqrt{5}-\alpha)/4\simeq-1.820$	$\frac{5+\sqrt{5}-\alpha}{4}$	$\frac{\sqrt{2}[6+2\sqrt{5}-(\sqrt{5}+1)\alpha]}{16}$	$\frac{\sqrt{2}[-4+8\sqrt{5}-(\sqrt{5}-1)\alpha]}{16}$	$\frac{95+5\sqrt{5}}{8}-\frac{(25+\sqrt{5})\alpha}{16}$	$\lvert\phi_n^-\rangle$
$(-3-\sqrt{5}+\beta)/4\simeq0.139$	$\frac{5-\sqrt{5}+\beta}{4}$	$\frac{\sqrt{2}[6-2\sqrt{5}-(\sqrt{5}-1)\beta]}{16}$	$\frac{\sqrt{2}[-4-8\sqrt{5}-(\sqrt{5}+1)\beta]}{16}$	$\frac{95-5\sqrt{5}}{8}+\frac{(25-\sqrt{5})\beta}{16}$	$\lvert\phi_n^-\rangle$
$(-3-\sqrt{5}-\beta)/4\simeq-2.757$	$\frac{5-\sqrt{5}-\beta}{4}$	$\frac{\sqrt{2}[6-2\sqrt{5}+(\sqrt{5}-1)\beta]}{16}$	$\frac{\sqrt{2}[-4-8\sqrt{5}+(\sqrt{5}+1)\beta]}{16}$	$\frac{95-5\sqrt{5}}{8}-\frac{(25-\sqrt{5})\beta}{16}$	$\lvert\phi_n^-\rangle$
2	0	-1	-1	3	$\lvert\varphi_n^+\rangle$
-1	-3	2	-1	15	$\lvert\varphi_n^+\rangle$
$(3+\sqrt{5})/2\simeq2.618$	$(-1+\sqrt{5})/2$	$(-1+\sqrt{5})/2$	$(3-\sqrt{5})/2$	$(15-5\sqrt{5})/2$	$\lvert\varphi_n^+\rangle$
$(3-\sqrt{5})/2\simeq0.382$	$(-1-\sqrt{5})/2$	$(-1-\sqrt{5})/2$	$(3+\sqrt{5})/2$	$(15+5\sqrt{5})/2$	$\lvert\varphi_n^+\rangle$
$(1+\sqrt{5})/2\simeq1.618$	$(-3+\sqrt{5})/2$	$(-1-\sqrt{5})/2$	$(1-\sqrt{5})/2$	$(15-3\sqrt{5})/2$	$\lvert\varphi_n^-\rangle$
$(1-\sqrt{5})/2\simeq-0.618$	$(-3-\sqrt{5})/2$	$(-1+\sqrt{5})/2$	$(1+\sqrt{5})/2$	$(15+3\sqrt{5})/2$	$\lvert\varphi_n^-\rangle$
$(1+\sqrt{17})/2\simeq2.562$	$(-3+\sqrt{17})/2$	$(5-\sqrt{17})/2$	$-4+\sqrt{17}$	$51-12\sqrt{17}$	$\lvert\varphi_n^-\rangle$
$(1-\sqrt{17})/2\simeq-1.562$	$(-3-\sqrt{17})/2$	$(5+\sqrt{17})/2$	$-4-\sqrt{17}$	$51+12\sqrt{17}$	$\lvert\varphi_n^-\rangle$

TABLE IV. The eigenvalues and the corresponding degree of degeneracy for C_{60} with a single-bond hopping-integral t_1 and a double-bond hopping-integral t_2. Note that $t_2 \simeq 1.1 t_1$. The characteristic polynomials from which those eigenvalues are solved are indicated in the left-hand column. Here $\tau=[16\,t_2^2-8(1+\sqrt{5})t_2t_1+10(3+\sqrt{5})t_1^2]$ and $\gamma=[16\,t_2^2-8(1-\sqrt{5})t_2t_1+10(3-\sqrt{5})t_1^2]$. Also η and ξ satisfy $(16\,t_2^3-24\,t_2^2t_1+12\,t_2t_1^2+25\,t_1^3)=54(\eta^3-3\eta\xi^2)$ and $[3\,(64\,t_2^4-160\,t_2^3t_1+288\,t_2^2t_1^2-200\,t_2t_1^3+125\,t_1^4)]=18\,(3\eta^2\xi-\xi^3)$. Notice that the fivefold degenerate HOMO (threefold degenerate LUMO) energy, as indicated, is solved from the polynomial constructed from the starting state $|\varphi_0\rangle$ ($|\phi_0\rangle$)—with negative parity—which consists of orbitals on two opposite hexagons (pentagons) with a threefold (fivefold) symmetry axis passing through their centers.

	Energy	Degeneracy
	$-(2t_1+t_2)$	1
	$-(t_1+t_2)/3+2\eta$	5
P_4^{p+}	$-(t_1+t_2)/3-\eta+\sqrt{3}\xi$	5
	$-(t_1+t_2)/3-\eta-\sqrt{3}\xi$	5
	$[(-3k+\sqrt{5})t_1+\tau]/4$	3
	$[(-3+\sqrt{5})t_1-\tau]/4$	3
P_4^{p-}	$[(-3-\sqrt{5})t_1+\gamma]/4$ (LUMO)	3
	$[(-3-\sqrt{5})t_1-\gamma]/4$	3
	$(t_1+\sqrt{5t_1^2+4t_2^2})/2$	4
	$(t_1-\sqrt{5t_1^2+4t_2^2})/2$	4
P_4^{h+}	$t_2+(1+\sqrt{5})t_1/2$	3
	$t_2+(1-\sqrt{5})t_1/2$	3
	$(t_1+\sqrt{5t_1^2-4t_1t_2+4t_2^2})/2$	5
P_4^{h-}	$(t_1-\sqrt{5t_1^2-4t_1t_2+4t_2^2})/2$ (HOMO)	5
	$(t_1+\sqrt{5t_1^2+8t_1t_2+4t_2^2})/2$	4
	$(t_1-\sqrt{5t_1^2+8t_1t_2+4t_2^2})/2$	4

TABLE V. The HOMO wave function $\mathscr{N}_\lambda^{-1}\Sigma_{n=0}^{3}P_n(E_\lambda)|\varphi_n^-\rangle$ and LUMO wave function $\mathscr{N}_\lambda^{-1}\Sigma_{n=0}^{3}P_n(E_\lambda)|\phi_n^-\rangle$ for C_{60} in terms of $t\simeq 1.1$. Recall that $P_0(E_\lambda)=1$. Here $|\varphi_n^-\rangle$ stands for $|\varphi_n\rangle$ with $\mathscr{P}=-1$ and $|\phi_n^-\rangle$ for $|\phi_n\rangle$ with $\mathscr{P}=-1$. Also $\gamma=\sqrt{16\,t^2+2\,(4\,t-5)(\sqrt{5}-1)}$.

HOMO	
E_λ	$(1-\sqrt{4\,t^2-4\,t+5})/2$
$P_1(E_\lambda)$	$-t-(1+\sqrt{4\,t^2-4\,t+5})/2$
$P_2(E_\lambda)$	$t-(3-\sqrt{4\,t^2-4\,t+5})/2$
$P_3(E_\lambda)$	$t-(1-\sqrt{4\,t^2-4\,t+5})/2$
$\mathscr{N}_\lambda^2$	$6\,t^2-6\,t-\frac{15}{2}+(3\,t-\frac{3}{2})\sqrt{4\,t^2-4\,t+5}$

LUMO	
E_λ	$(-3-\sqrt{5}+\gamma)/4$
$P_1(E_\lambda)$	$(5-\sqrt{5}+\gamma)/4t$
$P_2(E_\lambda)$	$\sqrt{2}[\,4(\sqrt{5}-1)t+10-6\sqrt{5}-(\sqrt{5}-1)\gamma]/16t$
$P_3(E_\lambda)$	$-\sqrt{2}[\,4(\sqrt{5}+1)t+4\sqrt{5}+(\sqrt{5}+1)\gamma]/16t$
$\mathscr{N}_\lambda^2$	$\dfrac{80\,t^2+40\,(\sqrt{5}-1)t+50\,(3-\sqrt{5})+(4\sqrt{5}t+25-5\sqrt{5})\gamma}{16\,t^2}$

H is applied l times to an initial $2p_z$ electron state $|j\rangle$, localized at carbon site j. Each time **H** is applied, the electron gains a certain amount of kinetic energy depending upon the bond (single or double) it travels. This enables the electron to hop through l bonds, reaching the final state $\mathbf{H}^l|j\rangle$. The moment $\mathscr{M}_l$ just equals the total kinetic energy gained by the electron returning to the starting site j after hopping l steps.

It is obvious that $\mathscr{M}_l$ will be zero when the l-hops path does not return to the starting site. In other words, $\mathscr{M}_l=0$ when there is no path of l hops for which the electron may return to the initial site. For the case $t=1$, the absolute value of the moment $\mathscr{M}_l$ is the total number of closed paths of l steps starting and ending at the same site. The spirit of this approach follows Feynman's program: to compute physical quantities from sums over paths.

The moments can be calculated analytically by hand, as well as by computer using a symbolic manipulation program. Below we describe these two implementations starting from the former. Let us first examine the action of the Hamiltonian on an arbitrary state $|j\rangle$. This results in three nearest-neighbor atom states with an additional factor accounting for the respective bond hopping energy. For example, $\mathbf{H}|1\rangle=(-t)|2\rangle+(-1)|3\rangle+(-1)|3''\rangle$ (labels as shown in Fig. 2). For simplicity and without any loss of generality, we choose orbital $|1\rangle$ to be our starting state. Now, for $l=1$, starting from vertex 1 and following the connectivity of C_{60} (Fig. 2), we write down the factors $-t$, -1, and -1 on the vertices 2, 3, and 3‴, respectively. A similar procedure holds for $l=2$. Starting from the three resulting vertices with respective factors, we then write down $(-t)(-1)=t$ on the vertices 4, 4′, 4″, and 4‴; $(-1)(-1)=1$ on the vertices 5 and 5″; and $(-1)(-1)+(-1)(-1)+(-t)(-t)=2+t^2$ on the vertex 1.

Our strategy here is as follows: each time the power of the (kinetic-energy) Hamiltonian increases by one, we move to

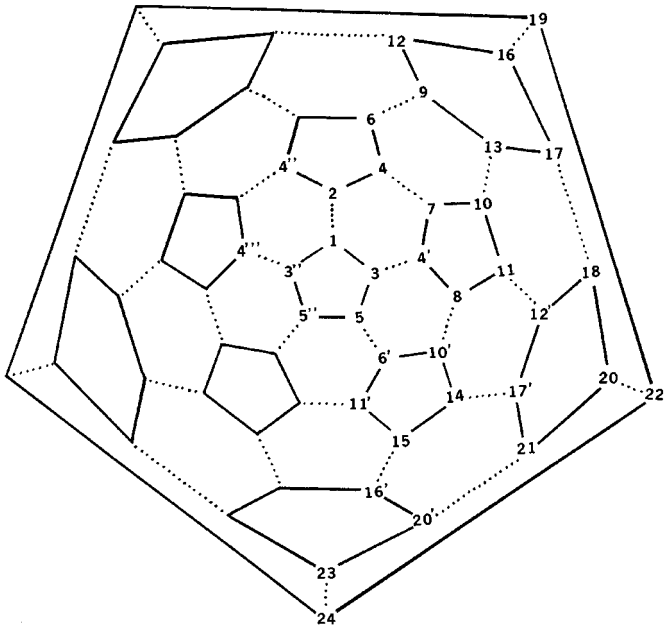

FIG. 2. Site labels used in the moments method. Independent vertices are those with j running from 1 to 24.

the adjacent nearest-neighboring vertices. Also the factor on each vertex is the sum of the factors on the three nearest-neighbor vertices times the bond hopping integral between vertices. It is then straightforward, with the aid of "the flattened C_{60} graph," to obtain all the factors on the available vertices for any power of the Hamiltonian. From its definition, it is evident that the moment of order l is just the factor on the vertex 1 for $\mathbf{H}^l$. For example, $\mathscr{M}_1=0$ (i.e., the number of closed paths obtained by moving one step is zero) and $\mathscr{M}_2=2+t^2$. By following this strategy, we can generate, one by one, all the moments to any order.

It is worthwhile to notice the mirror-symmetry between the left and right halves of C_{60} for the atom vertices and bonds. So we need only concern ourselves with the factors on the vertices in the right part. Furthermore, because of the geometrical equivalence, with respect to vertex 1, of eight pairs of vertices (j and j' in Fig. 2), the total number of independent vertices can be reduced to 24. All calculations up to this point can be done analytically by hand.

An alternative analogous procedure can be implemented by using symbolic manipulation software on a computer. First, we define an auxiliary quantity,[11] $W_l(j)$, which is the sum over all possible paths of l steps on which an electron may hop from the vertex 1 to the vertex j. From the connectivity of C_{60}, we can then construct 24 independent recurrence relations. For instance, $W_{l+1}(1)=-tW_l(2)-2W_l(3)$, $W_{l+1}(2)=-tW_l(1)-2W_l(4)$, and $W_{l+1}(3)=-tW_l(4)-W_l(1)-W_l(5)$. The recurrence relations state that the vertex j can be reached by taking the (l+1)th step from the three nearest-neighbor vertices. The factors $-t$ and -1 account for the connecting bond-hopping integral. With the initial conditions $W_0(1)=1$ and $W_0(j)=0$ for the rest of j's, we can obtain the moments to any order as $\mathscr{M}_l=W_l(1)$. We list $\mathscr{M}_3$ through $\mathscr{M}_9$ here: 0, t^4+8t^2+6, -2, $t^6+18t^4+4t^3+48t^2+20$, $-14t^2-14$, $t^8+32t^6+16t^5+184t^4+48t^3+256t^2+70$, and $-54t^4-18t^3-162t^2-72$, for $l=3,4,\ldots,9$. The moments $\mathscr{M}_{10}$ through $\mathscr{M}_{32}$ (the highest order moment needed to obtain the entire energy spectrum) are not presented here.

The correctness of the calculated moments $\mathscr{M}_l$ is assured by the consistency of the results from these two approaches. It is evident that through these two implementations we can also obtain the quantities $\langle 1|\mathbf{H}^l|j\rangle$ for $j\neq 1$ which can be appropriately interpreted as the "*sum-over-paths*" between sites 1 and j. For instance, $\langle 1|\mathbf{H}^l|j\rangle$ just equals $W_l(j)$.

To obtain the energy spectrum, we again utilize Eq. (7). So the next step is to express the parameters a_n and b_{n+1} in terms of the moments. We employ the following formulas:[12] define the auxiliary matrix M with the first row elements defined as $M_{0,l}\equiv\mathscr{M}_l$. The other rows are evaluated by using only one immediate predecessor row:

$$M_{n,l}=\frac{M_{n-1,l+2}-M_{n-1,1}M_{n-1,l+1}}{M_{n-1,2}-M_{n-1,1}^2}-\sum_{k=0}^{l-1}M_{n,k}M_{n-1,l-k},$$

$$n\geq 1;\ l=0,1,\ldots. \quad (14)$$

The a_n's and b_{n+1}'s are obtained from the elements of the second and third columns as

TABLE VI. Parameters a_n and b_n for $n=0,1,\ldots,9$ calculated from the moments $\mathscr{M}_l$ with $t=1$ in the moment method for C_{60}. Numbers in the denominator are relatively prime to those in numerator and all numbers in square root are primes.

n	a_n	b_n
0	0	
1	0	$\sqrt{3}$
2	$-\frac{1}{3}$	$\sqrt{2}$
3	$\frac{11}{69}$	$\frac{1}{3}\sqrt{23}$
4	$-\frac{6633}{10\,925}$	$\frac{5}{23}\sqrt{2\times 19}$
5	$-\frac{1\,109\,069}{2\,724\,600}$	$\frac{6}{475}\sqrt{2\times 23\times 239}$
6	$-\frac{52\,107\,413}{684\,218\,760}$	$\frac{5}{5736}\sqrt{5\times 19\times 23857}$
7	$-\frac{66\,333\,080\,317}{113\,465\,204\,135}$	$\frac{12}{119\,285}\sqrt{23\times 239\times 41357}$
8	$-\frac{23\,875\,175\,834\,189}{52\,324\,285\,077\,614}$	$\frac{1}{2\,853\,633}\sqrt{3\times 5\times 11\times 31\times 80657\times 23857}$
9	$\frac{603\,116\,478\,351\,886\,109}{1\,730\,319\,460\,378\,457\,102}$	$\frac{23}{165\,024\,222}\sqrt{3\times 7\times 17\times 41357\times 11492779}$

$$a_n=M_{n,1} \quad (15)$$

and

$$b_{n+1}^2=M_{n,2}-M_{n,1}^2, \quad (16)$$

here $n=0,1,2,\ldots$. Note that elements in the first column $M_{n,0}$ are always equal to 1.

We find analytically that b_{15}^2 *exactly* equals 0 for $t=1$ and b_{16}^2 *exactly* equals 0 for an arbitrary t. Below we discuss the $t=1$ case and similar results can be obtained for $t\neq 1$. The exact vanishing of b_{15}^2, in the case $t=1$, indicates the truncation at b_{15}. Thus, we expect 15 eigenvalues. It also turns out that the highest order of moment we need is $l=30$. The moments $\mathscr{M}_4$ through $\mathscr{M}_{20}$ for $t=1$ are 15, -2, 91, -28, 607, -306, 4274, -3080, 31 227, $-29\,718$, 234 559, $-279\,100$, 1 803 375, $-2\,572\,542$, 14 149 891, $-23\,398\,880$, and 113 056 535. The moments $\mathscr{M}_{21}$ through $\mathscr{M}_{30}$ were computed but are not shown here. Through the calculated parameters $\{a_0,a_1,\ldots,a_{14}\}$ and $\{b_1,b_2,\ldots,b_{14}\}$ (we only present $\{a_0,\ldots,a_9\}$ and $\{b_1,\ldots,b_9\}$ in Table VI), we can construct the polynomial $P_{15}(E)$ by using Eq. (7). By solving $P_{15}(E)=0$, we thus obtain 15 energy levels. The results are exactly identical to those obtained from the recursion method approach.

B. Alternative application of the moments method

In the above description of the moments approach, the main ingredient is the computation of the moments for a natural choice of state $|1\rangle$ centered at the atom labeled by 1. However, it is worthwhile to incorporate the inversion symmetry property. Therefore, instead of focusing on a single localized state, we turn to the computation of the moments with respect to states

$$|I_\pm\rangle=\frac{1}{\sqrt{2}}(|1\rangle\pm|24\rangle), \quad (17)$$

where atoms labeled by 1 and 24 in Fig. 2 are antipodes. It is a simple exercise to construct the following identity for the moments defined by $\langle I_\pm|\mathbf{H}^l|I_\pm\rangle$,

$$\langle I_\pm|\mathbf{H}^l|I_\pm\rangle=\langle 1|\mathbf{H}^l|1\rangle\pm\langle 1|\mathbf{H}^l|24\rangle. \quad (18)$$

TABLE VII. Parameters a_n and b_n computed from the moments $\langle I_\pm|\mathbf{H}^l|I_\pm\rangle$ with $t=1$.

	From $\langle I_+\|\mathbf{H}^l\|I_+\rangle$		From $\langle I_-\|\mathbf{H}^l\|I_-\rangle$	
n	a_n	b_n	a_n	b_n
0	0		0	
1	0	$\sqrt{3}$	0	$\sqrt{3}$
2	$-\frac{1}{3}$	$\sqrt{2}$	$-\frac{1}{3}$	$\sqrt{2}$
3	$\frac{11}{69}$	$\frac{1}{3}\sqrt{23}$	$\frac{11}{69}$	$\frac{1}{3}\sqrt{23}$
4	$-\frac{18\,027}{21\,850}$	$\frac{5}{23}\sqrt{2\times19}$	$-\frac{1701}{4370}$	$\frac{5}{23}\sqrt{2\times19}$
5	$-\frac{1\,964\,421}{36\,832\,450}$	$\frac{1}{950}\sqrt{3\times23\times137\times283}$	$-\frac{11\,563}{44\,650}$	$\frac{1}{190}\sqrt{3\times5\times23\times47}$
6	$\frac{40\,798}{38\,771}$	$\frac{855}{38\,771}\sqrt{2\times3\times13\times19}$	$\frac{342\,588}{22\,258\,025}$	$\frac{19}{1175}\sqrt{2\times997}$
7			$-\frac{3661}{18\,943}$	$\frac{100}{18\,943}\sqrt{17\times47\times89}$

These moments can then be readily obtained since the quantities $\langle 1|\mathbf{H}^l|1\rangle$ and $\langle 1|\mathbf{H}^l|24\rangle$ are already available. Note that the lowest order for the appearance of a nonzero $\langle 1|\mathbf{H}^l|24\rangle$ is $l=9$. This is because the shortest path for vertex 1 to reach vertex 24 contains 9 steps. We thus obviously have $\langle I_\pm|\mathbf{H}^l|I_\pm\rangle=\mathscr{M}_l$ for $l\leqslant 8$.

For the case $t=1$, the highest order we need for $\langle I_+|\mathbf{H}^l|I_+\rangle$ ($\langle I_-|\mathbf{H}^l|I_-\rangle$) is $l=14$ (16), because b_7^2 (b_8^2) calculated from the moment $\langle I_+|\mathbf{H}^l|I_+\rangle$ ($\langle I_-|\mathbf{H}^l|I_-\rangle$) gives exactly 0. Through the computed parameters $\{a_0,\ldots,a_6\}$ and $\{b_1,\ldots,b_6\}$ ($\{a_0,\ldots,a_7\}$ and $\{b_1,\ldots,b_7\}$), we *analytically* obtain 7 (8) eigenvalues which are identical to those belonging to the $\mathscr{P}=+1$ ($\mathscr{P}=-1$) category from the recursion method. The moments $\langle I_+|\mathbf{H}^l|I_+\rangle$, for $l=9,\ldots,14$, are -312, 4319, -3278, 32 339, $-33\,436$, and 252 339. Also the moments $\langle I_-|\mathbf{H}^l|I_-\rangle$ are -300, 4231, -2882, 30 115, $-26\,000$, 216 779, $-225\,080$, and 1 571 823, respectively, for $l=9,\ldots,16$. Their respective set of parameters a_n's and b_{n+1}'s are presented in Table VII. The result that a_n and b_{n+1} for $n=0,1,2$, and 3 in Table VII are identical to those in Table VI comes from the fact $\langle I_\pm|\mathbf{H}^l|I_\pm\rangle=\mathscr{M}_l$ for $l\leqslant 8$.

For an arbitrary t, we need the moments $\langle I_\pm|\mathbf{H}^l|I_\pm\rangle$ up to order 16. The moments $\langle I_\pm|\mathbf{H}^9|I_\pm\rangle$ through $\langle I_\pm|\mathbf{H}^{13}|I_\pm\rangle$ are listed in Table VIII, while $\langle I_\pm|\mathbf{H}^{14}|I_\pm\rangle$, $\langle I_\pm|\mathbf{H}^{15}|I_\pm\rangle$, and $\langle I_\pm|\mathbf{H}^{16}|I_\pm\rangle$ were computed but are not presented here. We analytically find that b_8^2 calculated from these two sets of moments *exactly* equals 0 in both cases. Consequently, consistent results for the eigenvalues are recovered.

In this section, we have presented an unconventional choice of initial states and concentrated on the moments with respect to these states. It is shown that this approach is even more efficient in analytically obtaining the energy eigenvalues.

V. RELATIONSHIP BETWEEN THE RECURSION AND MOMENTS METHODS

Generally speaking, the moments method is closely related to the recursion method, especially in the aspect that both methods lead to the same results for the parameters a_n and b_{n+1}^2. In this section, we illustrate this point by showing that the same expressions for the parameters in the recursion method case $\mathscr{B}$ can be obtained through the moments method. As the initial states are $|\phi_0\rangle$ and $|\varphi_0\rangle$ in this case

TABLE VIII. Moments (sums over paths) $\langle I_\pm|\mathbf{H}^l|I_\pm\rangle$, with an arbitrary t, for $l=9,\ldots,13$.

Order (l)	Moment ($\langle I_+\|\mathbf{H}^l\|I_+\rangle$)
9	$-54\,t^4-24\,t^3-162\,t^2-72$
10	$t^{10}+50\,t^8+40\,t^7+500\,t^6+304\,t^5$ $+1490\,t^4+400\,t^3+1280\,t^2+254$
11	$-154\,t^6-176\,t^5-990\,t^4-396\,t^3-1232\,t^2-330$
12	$t^{12}+72\,t^{10}+80\,t^9+1110\,t^8+1104\,t^7+5784\,t^6$ $+3648\,t^5+10560\,t^4+2840\,t^3+6192\,t^2+948$
13	$-364\,t^8-728\,t^7-4212\,t^6-4056\,t^5$ $-10920\,t^4-3952\,t^3-7774\,t^2-1430$
Order (l)	Moment ($\langle I_-\|\mathbf{H}^l\|I_-\rangle$)
9	$-54\,t^4-12\,t^3-162\,t^2-72$
10	$t^{10}+50\,t^8+40\,t^7+500\,t^6+296\,t^5$ $+1450\,t^4+360\,t^3+1280\,t^2+254$
11	$-154\,t^6-88\,t^5-902\,t^4-176\,t^3-1232\,t^2-330$
12	$t^{12}+72\,t^{10}+80\,t^9+1110\,t^8+1056\,t^7+5596\,t^6$ $+3120\,t^5+9840\,t^4+2200\,t^3+6192\,t^2+948$
13	$-364\,t^8-364\,t^7-3484\,t^6-1716\,t^5$ $-9256\,t^4-1612\,t^3-7774\,t^2-1430$

$\mathscr{B}$, the moments we now need to compute are $\langle\phi_0|\mathbf{H}^l|\phi_0\rangle$ and $\langle\varphi_0|\mathbf{H}^l|\varphi_0\rangle$. It is straightforward to find that

$$\langle\phi_0|\mathbf{H}^l|\phi_0\rangle=\langle 1|\mathbf{H}^l|1\rangle+2\langle 1|\mathbf{H}^l|3\rangle+2\langle 1|\mathbf{H}^l|5\rangle +\mathscr{P}(\langle 1|\mathbf{H}^l|24\rangle+2\langle 1|\mathbf{H}^l|22\rangle+2\langle 1|\mathbf{H}^l|19\rangle) \tag{19}$$

and

$$\langle\varphi_0|\mathbf{H}^l|\varphi_0\rangle=\langle 1|\mathbf{H}^l|1\rangle-\langle 1|\mathbf{H}^l|2\rangle-\langle 1|\mathbf{H}^l|3\rangle-\langle 1|\mathbf{H}^l|7\rangle +2\langle 1|\mathbf{H}^l|4\rangle +\mathscr{P}(\langle 1|\mathbf{H}^l|24\rangle-\langle 1|\mathbf{H}^l|23\rangle-\langle 1|\mathbf{H}^l|22\rangle -\langle 1|\mathbf{H}^l|21\rangle+2\langle 1|\mathbf{H}^l|20\rangle). \tag{20}$$

Notice that the site labels on the right-hand sides of the above two equations refer to Fig. 2. Through the techniques for the calculation of these quantities previously discussed, the moments $\langle\phi_0|\mathbf{H}^l|\phi_0\rangle$ and $\langle\varphi_0|\mathbf{H}^l|\varphi_0\rangle$ can be readily obtained.

Anticipating the termination at b_4^2, we only need these moments up to order 8. In Table IX we give the moments with respect to $|\phi_0\rangle$ and $|\varphi_0\rangle$. By utilizing Eqs. (14)–(16), we thus obtain a_n's and b_{n+1}^2's which are consistent with those (in Table II) derived directly from the recursion method. To illustrate this consistency, we explicitly present here the results for the b_{n+1}^2's. From $\langle\phi_0|\mathbf{H}^l|\phi_0\rangle$, we have

TABLE IX. Moments (sums over paths) $\langle\phi_0|\mathbf{H}^l|\phi_0\rangle$ and $\langle\varphi_0|\mathbf{H}^l|\varphi_0\rangle$ for $l=1,\ldots,8$.

Order (l)	Moment $\langle\phi_0|\mathbf{H}^l|\phi_0\rangle$
1	-2
2	t^2+4
3	$-4t^2-8$
4	t^4+14t^2+16
5	$-6t^4-2t^3-40t^2-32$
6	$t^6+30t^4+8t^3+110t^2+64$
7	$-8t^6-6t^5-112t^4-(36+2\mathscr{P})t^3-282t^2-128$
8	$t^8+52t^6+32t^5+(396+4\mathscr{P})t^4$ $+(116+12\mathscr{P})t^3+708t^2+256$

Order (l)	Moment $\langle\varphi_0|\mathbf{H}^l|\varphi_0\rangle$
1	$t+1$
2	t^2+2t+2
3	t^3+3t^2+5t+3
4	$t^4+4t^3+10t^2+10t+5$
5	$t^5+5t^4+16t^3+25t^2+20t+8$
6	$t^6+6t^5+24t^4+48t^3+60t^2+38t+13$
7	$t^7+7t^6+33t^5+84t^4+(133+\mathscr{P})t^3$ $+133t^2+71t+21$
8	$t^8+8t^7+44t^6+132t^5+(266+2\mathscr{P})t^4$ $+(336+4\mathscr{P})t^3+284t^2+130t+34$

$b_1^2=t^2$, $b_2^2=2$, $b_3^2=1$, and $b_4^2=(1-\mathscr{P}^2)t^2=0$. From $\langle\varphi_0|\mathbf{H}^l|\varphi_0\rangle$, we have $b_1^2=1$, $b_2^2=t^2$, $b_3^2=1$, and $b_4^2=(1-\mathscr{P}^2)t^2=0$. We thus demonstrate the fact that the same results for the parameters a_n and b_{n+1}^2 can be obtained by using either the recursion or moments methods. The advantage of the recursion method lies in the fact that we can simultaneously generate the states and the parameters. However, it is sometimes difficult to derive the states and parameters when the recursion method is applied to some starting state, for example, a single carbon atom state $|j\rangle$, while the moment method provides standard procedures to calculate the parameters after the moments are obtained.

VI. LOCAL DENSITY OF STATES

In the recursion and moments methods, the diagonal element of the Green function $(E-\mathbf{H})^{-1}$ can be expressed as a continued fraction[8,12]

$$G_0(E)=\left\langle f_0\left|\frac{1}{E-\mathbf{H}}\right|f_0\right\rangle = \cfrac{1}{E-a_0-\cfrac{b_1^2}{E-a_1-\cfrac{b_2^2}{E-a_2-\cdots-\cfrac{b_{N-1}^2}{E-a_{N-1}}}}}. \tag{21}$$

The local density of states $\rho(E)$ for $|f_0\rangle$ is related to the imaginary part of $G_0(E)$ by

$$\rho(E)=\lim_{\varepsilon\to 0}-\frac{1}{\pi}\mathrm{Im}G_0(E+i\varepsilon). \tag{22}$$

From the computational point of view, $G_0(E)$ can be obtained by iteratively applying the following transformation:

$$G_n(E)=\frac{1}{E-a_n-b_{n+1}^2G_{n+1}(E)},$$

starting from $G_{N-1}(E)=1/(E-a_{N-1})$. By substituting the parameters a_n and b_{n+1}^2 from either one of the two methods into Eq. (21) and using Eq. (22), we thus obtain the local density of states on several initial states. In our two alternative applications of the recursion method, we have used four different starting states: $|u_0\rangle$, $|v_0\rangle$, $|\phi_0\rangle$, and $|\varphi_0\rangle$. Their $G_0(E)$'s can be written explicitly as

$$G_0^{-1}=E+2-t^2\{E-2[E+t-(E+1+\mathscr{G}_p)^{-1}]^{-1}\}^{-1} \tag{23}$$

and

$$G_0^{-1}=E-t-1-\{E-t^2[E-1-(E-\mathscr{G}_h)^{-1}]^{-1}\}^{-1}, \tag{24}$$

where

$$\mathscr{G}_p=\begin{cases}\mathscr{P}t & \text{for the state } |\phi_0\rangle\\ -t^2(E+1-\{E+t-2[E-t^2(E+2)^{-1}]^{-1}\}^{-1})^{-1} & \text{for the state } |u_0\rangle\end{cases}$$

and

$$\mathscr{G}_h=\begin{cases}\mathscr{P}t & \text{for the state } |\varphi_0\rangle\\ t^2(E-\{E-1-t^2[E-(E-t-1)^{-1}]^{-1}\}^{-1})^{-1} & \text{for the state } |v_0\rangle.\end{cases}$$

The LDOS around these ring-clusters are plotted in Fig. 3 and Fig. 4. Notice that around a pentagon (hexagon) ring the LDOS is large at low (high) energies. This is related to the fact that a pentagon (hexagon) has zero (three) double bonds and five (three) single bonds. Also from the moments approach, the local density of states on two antipode carbon atoms are plotted in Fig. 5. In principle, they are experimentally accessible by using a scanning tunneling microscope.[9] In one of the moments method approaches, the initial state is a $2p_z$ orbital on a carbon atom. The local density of states in the case $t=1$ is plotted in Fig. 6. From Fig. 6, we can obtain the degree of degeneracy for each energy level, which is the respective LDOS value times 2. The common factor of 2 comes from the consideration that the total number of π electrons is 60. For $t\neq 1$, conclusions for the degeneracy can be similarly drawn.

VII. SOLUTION FOR THE ELECTRONIC σ STATES

It is apparent that the Hamiltonian $\mathbf{H}_\sigma$ is more complex than $\mathbf{H}_\pi$ due to the two different couplings. However, an analytic transformation of this Hamiltonian into a simpler one with a single "renormalized" hopping parameter between sites can be established.[10] The energy states can then be readily solved. Below we first present the transformation of the σ-states Hamiltonian into a π-type one. As a consequence, the resulting solutions of the eigenvalues for the σ states are obtained.

We first write the σ states eigenfunctions as

$$|\Psi_\sigma\rangle=\sum_i \mathscr{C}_i|i,\alpha\rangle, \tag{25}$$

where $\mathscr{C}=a,b,$ and c represents, respectively, the corresponding coefficient for the orbital $\alpha=sp_a^2,sp_b^2,$ and sp_c^2 at each site i. Let us now focus attention on a given atom labeled i. Also let atoms $j,k,$ and l be the three adjacent nearest neighbors of the i atom. The energy eigenvalue equation $\mathbf{H}_\sigma|\Psi_\sigma\rangle=\epsilon|\Psi_\sigma\rangle$ then reads

$$\epsilon a_i=-V_2a_j-V_1(b_i+c_i), \tag{26}$$

$$\epsilon b_i=-V_2c_k-V_1(a_i+c_i), \tag{27}$$

$$\epsilon c_i=-V_2b_l-V_1(a_i+b_i), \tag{28}$$

and

$$\epsilon a_j=-V_2a_i-V_1(b_j+c_j), \tag{29}$$

$$\epsilon c_k=-V_2b_i-V_1(a_k+b_k), \tag{30}$$

$$\epsilon b_l=-V_2c_i-V_1(a_l+c_l), \tag{31}$$

and so on. We then define

$$A_i=a_i+b_i+c_i \tag{32}$$

as the sum of the coefficients for orbitals at the site i, and

$$B_i=a_j+c_k+b_l \tag{33}$$

as the sum of the coefficients for orbitals on the bonds associated with the site i. Similar equations hold for the other A's and B's. In the first place, Eqs. (26) and (29) can be rewritten as

$$(\epsilon-V_1)a_i+V_2a_j=-V_1A_i \tag{34}$$

and

$$V_2a_i+(\epsilon-V_1)a_j=-V_1A_j\,. \tag{35}$$

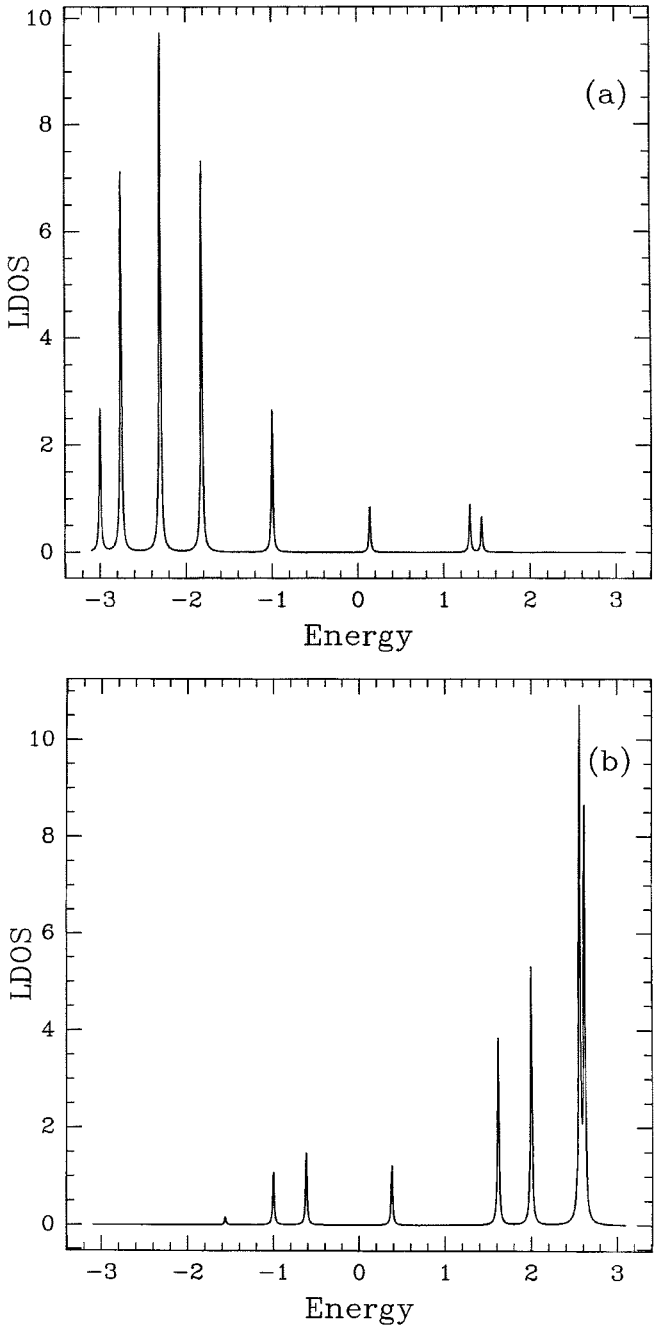

FIG. 3. The local density of states around ring clusters: (a) a pentagon, (b) a hexagon. They are obtained by using the recursion method. Notice that around a pentagon (hexagon) ring the LDOS is large at low (high) energies. This is related to the fact that a pentagon (hexagon) has zero (three) double bonds and five (three) single bonds.

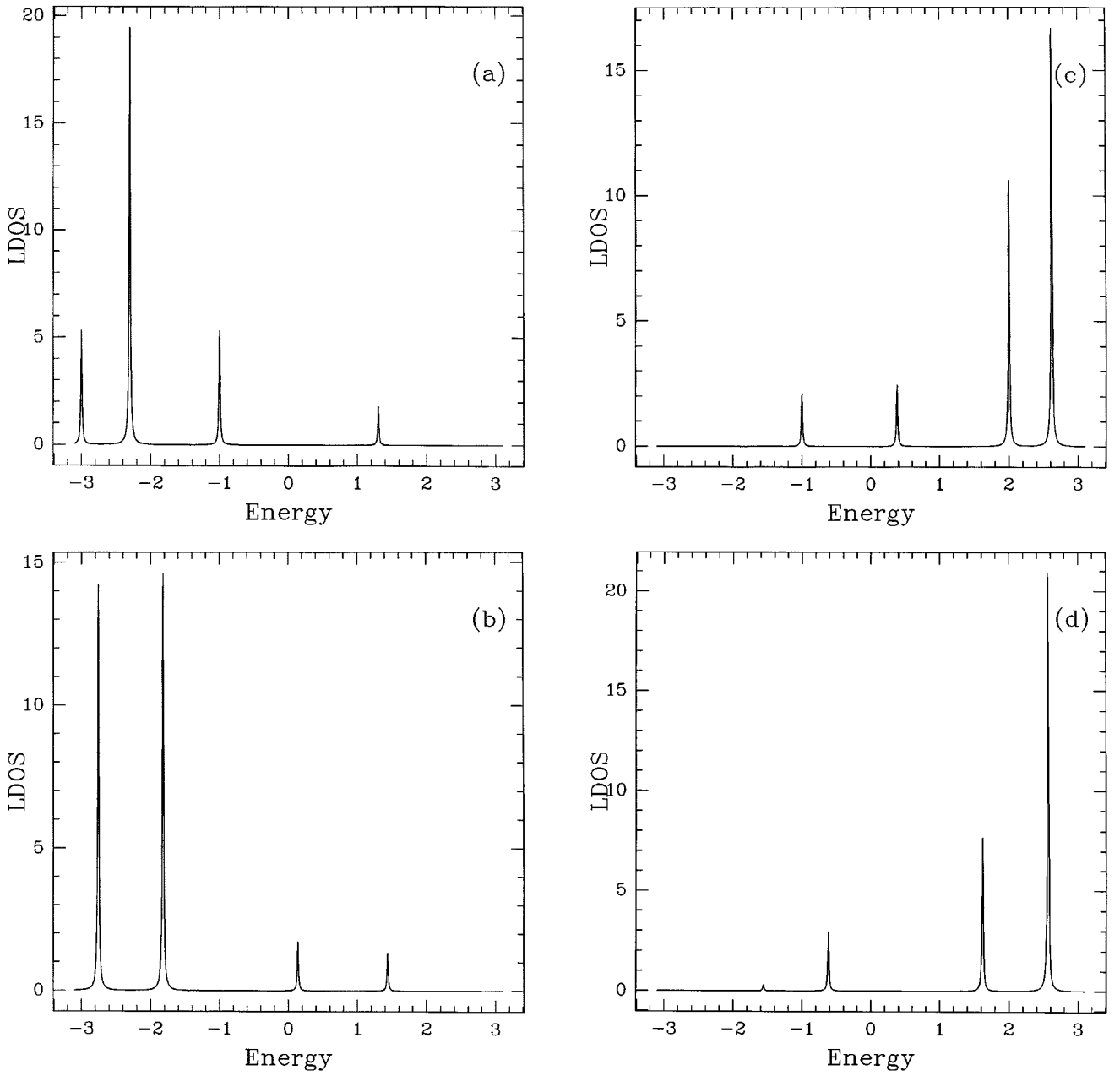

FIG. 4. The local density of states around two opposite (i.e., antipodes) pentagons with (a) even parity, (b) odd parity, and two opposite hexagons with (c) even parity, (d) odd parity. They are obtained by using the recursion method. Notice that around two antipode pentagon (hexagon) rings the LDOS is large at low (high) energies.

When the situation $A_i=A_j=0$ occurs, the secular equation immediately yields

$$\epsilon=V_1\pm V_2. \tag{36}$$

In all, there are 30 pairs of similar equation sets. We thus have two energy levels: V_1-V_2 belonging to the bonding states, and V_1+V_2 belonging to the antibonding states, each having a degree of degeneracy equal to 30. Furthermore, by respectively summing up Eqs. (26) through (28) and Eqs. (29) through (31), we have

$$\epsilon A_i=-V_2B_i-2V_1A_i \tag{37}$$

and

$$(\epsilon-V_1)B_i=-V_2A_i-V_1(A_j+A_k+A_l). \tag{38}$$

By substituting Eq. (37) into Eq. (38), we obtain

$$[(\epsilon+2V_1)(\epsilon-V_1)-V_2^2]A_i=V_1V_2(A_j+A_k+A_l). \tag{39}$$

It can be directly recognized that Eq. (39) is entirely equivalent to the problem of a tight-binding Hamiltonian with one state per atom and a single nearest-neighbor hopping integral, whose eigenvalue and eigenvector solutions are already fully explored in previous sections. Let E_λ ($\lambda=1,2,\ldots,15$) stand for the eigenvalues listed in Table III. It follows then that

$$(\epsilon_\lambda+2V_1)(\epsilon_\lambda-V_1)-V_2^2=V_1V_2E_\lambda. \tag{40}$$

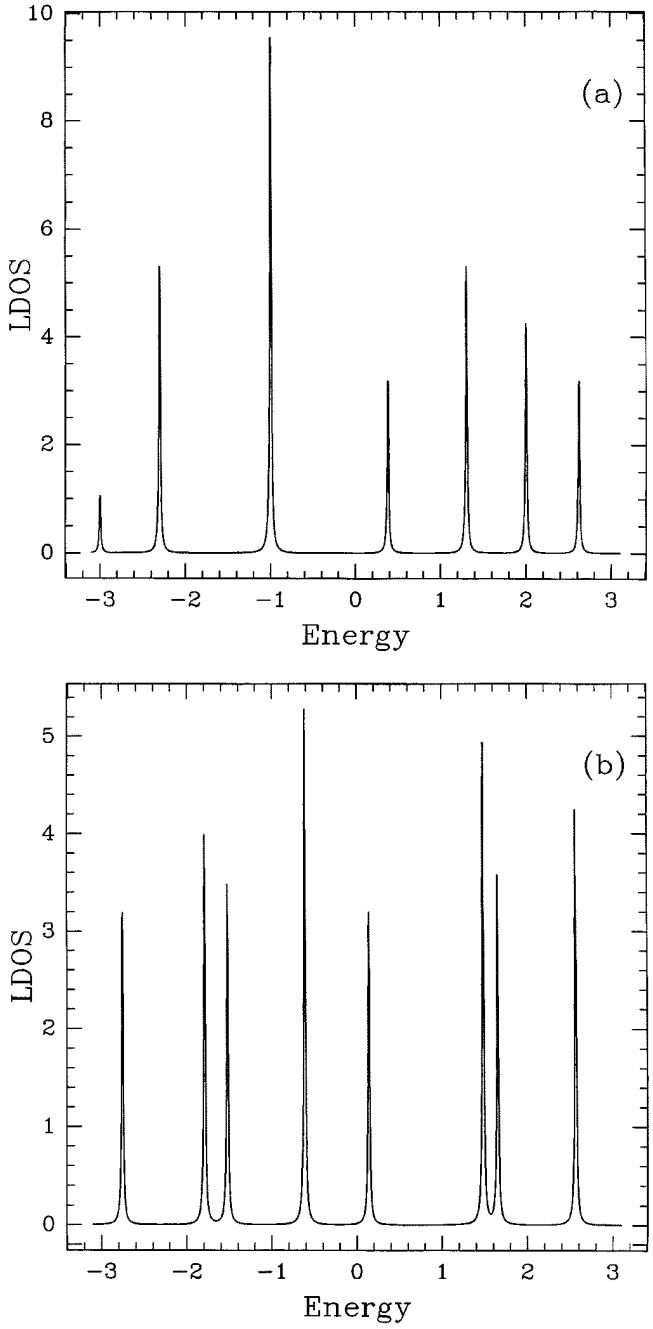

FIG. 5. The local density of states on two opposite carbon atoms (antipodes) with (a) even parity, (b) odd parity. They are obtained by using the moments method. Notice that there are seven even-parity solutions in (a) and eight different odd-parity solutions in (b); for a total of 15 different energy levels (for $t=1$).

Thus, we obtain

$$\epsilon_\lambda = -\frac{V_1}{2} \pm \sqrt{\frac{V_1^2}{4} + 2V_1^2 + V_2^2 + V_1 V_2 E_\lambda}$$

$$= -\frac{V_1}{2} \pm V_2 \sqrt{1 + \frac{V_1}{V_2} E_\lambda + \frac{9V_1^2}{4V_2^2}}\,. \tag{41}$$

The minus sign designates the bonding states, and the plus sign designates the antibonding states.

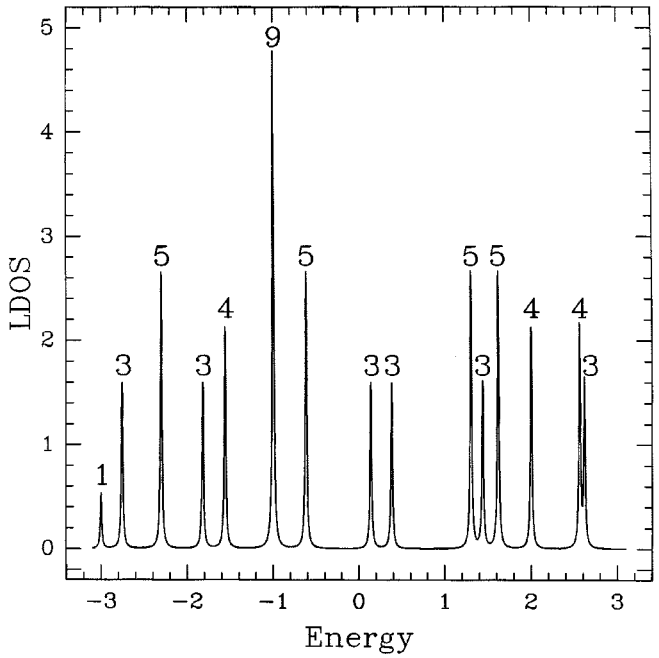

FIG. 6. The local density of states for a carbon atom obtained from the moments method with the respective degree of degeneracy shown above each peak.

Summarizing, in this section we obtain 90 bonding σ states and 90 antibonding σ states. Among the bonding (antibonding) states, 30 states are lumped together at the energy level $V_1 - V_2$ ($V_1 + V_2$). The other 60 σ bonding and 60 σ antibonding states are closely related to the energy spectrum for the π states. Finally, in the limit $V_2 \gg V_1$, we have

$$\epsilon_\lambda \simeq -\frac{V_1}{2} \pm V_2 \pm \frac{V_1}{2} E_\lambda\,. \tag{42}$$

It is also straightforward to obtain the corresponding eigenvector for an eigenvalue ϵ_λ. Since all the A_i's are already known, the initial coefficients a_i, b_i, and c_i can be calculated.

VIII. CONCLUSION

In conclusion, we use several approaches based on the recursion and moments methods in order to explore the electronic structure of a C_{60} molecule, obtaining exact closed-form expressions for the π and σ eigenvalues and eigenfunctions, including the HOMO and LUMO states, as well as the Green's functions and LDOS through alternative methods. These quantities are relevant to the several important experimental techniques which probe the local spectroscopy of molecules; for instance, by using a scanning tunneling microscope, as described in the review in Ref. 9. For comparison purposes, we have also done a direct numerical diagonalization of the full Hamiltonian and the results obtained are consistent with those from the previous analytical methods. However, the much more elegant and powerful recursion and moments methods provide valuable insights and closed-form expressions for various quantities characterizing the elec-

tronic structure of C_{60}. Finally, a generalized version of the recursion method can be used to greatly simplify the calculation of the electronic properties of large C_{60n^2} fullerenes (i.e., C_{240}, C_{540}, C_{960}, C_{1500}, C_{2160}, and C_{2940}).[13]

ACKNOWLEDGMENTS

The authors gratefully acknowledge stimulating and useful discussions with C. N. Yang and F. Guinea. F.N. acknowledges partial support from GE and a Rackham grant.

APPENDIX A: ORIGIN OF V_1 AND V_2

In this appendix we examine more closely the physical interpretation for the hopping integrals V_1 and V_2. Let $|i,\alpha\rangle$ be a hybrid orbital located at site i. We have

$$|i,sp_a^2\rangle = a_s^i|2s\rangle + a_x^i|2p_x\rangle + a_y^i|2p_y\rangle, \tag{A1}$$

$$|i,sp_b^2\rangle = b_s^i|2s\rangle + b_x^i|2p_x\rangle + b_y^i|2p_y\rangle, \tag{A2}$$

and

$$|j,sp_a^2\rangle = a_s^j|2s\rangle + a_x^j|2p_x\rangle + a_y^j|2p_y\rangle, \tag{A3}$$

where i and j are nearest neighbors. We also assume that orbitals $|i,sp_a^2\rangle$ and $|j,sp_a^2\rangle$ lie along the bond connecting i and j. It is straightforward to obtain

$$-V_1 = \langle i,sp_a^2|\mathbf{H}_\sigma|i,sp_b^2\rangle = a_s^{i*}b_s^i\epsilon_s + (a_x^{i*}b_x^i + a_y^{i*}b_y^i)\epsilon_p \tag{A4}$$

and

$$\begin{aligned} -V_2 &= \langle i,sp_a^2|\mathbf{H}_\sigma|j,sp_a^2\rangle \\ &= a_s^{i*}a_s^j t_{ss} + a_x^{i*}a_x^j t_{p_xp_x} + a_y^{i*}a_y^j t_{p_yp_y} \\ &\quad + (a_s^{i*}a_x^j + a_x^{i*}a_s^j)t_{sp_x} + (a_s^{i*}a_y^j + a_y^{i*}a_s^j)t_{sp_y} \\ &\quad + (a_x^{i*}a_y^j + a_y^{i*}a_x^j)t_{p_xp_y}. \end{aligned} \tag{A5}$$

Here ϵ_s and ϵ_p are the $2s$-level and $2p$-level energies and the t's are hopping matrix elements between orbitals on nearest-neighboring sites. It is evident that, with a suitable choice of a local coordinate system, we can always have

$$\langle i,sp_a^2|\mathbf{H}_\sigma|i,sp_b^2\rangle = \langle i,sp_a^2|\mathbf{H}_\sigma|i,sp_c^2\rangle = \langle i,sp_b^2|\mathbf{H}_\sigma|i,sp_c^2\rangle \tag{A6}$$

and

$$\langle i,sp_a^2|\mathbf{H}_\sigma|j,sp_a^2\rangle = \langle i,sp_b^2|\mathbf{H}_\sigma|k,sp_c^2\rangle = \langle i,sp_c^2|\mathbf{H}_\sigma|l,sp_b^2\rangle. \tag{A7}$$

In the above equation, we have assumed that orbitals $|i,sp_b^2\rangle$, $|k,sp_c^2\rangle$ lie along the bond connecting i and k and orbitals $|i,sp_c^2\rangle$, $|l,sp_b^2\rangle$ along the bond connecting i and l.

APPENDIX B: CALCULATION OF $\mathbf{H}|\phi_3\rangle$ AND $\mathbf{H}|\varphi_3\rangle$

In this appendix we present the calculation of the recurrence relations for states $|\phi_3\rangle$ and $|\varphi_3\rangle$ in the recursion method case $\mathscr{B}$. It is shown that the recurrence terminates at these states and two solutions for a_3 are constructed from each state. First,

$$\begin{aligned} \mathbf{H}|\phi_3\rangle &= \frac{1}{\sqrt{20}}\sum_{j=11}^{20}(|j\rangle + \mathscr{P}|j'\rangle) + \frac{1}{\sqrt{20}}\left[\sum_{j=21}^{30}(|j\rangle + t|j'\rangle) + \mathscr{P}\sum_{j=21}^{30}(t|j\rangle + |j'\rangle)\right] \\ &= |\phi_2\rangle - \left[-\frac{1}{\sqrt{20}}\sum_{j=21}^{30}[(1+\mathscr{P}t)|j\rangle + (t+\mathscr{P})|j'\rangle]\right] \\ &= |\phi_2\rangle - \left[-\frac{1}{\sqrt{20}}\sum_{j=21}^{30}[(1+\mathscr{P}t)|j\rangle + (1+\mathscr{P}t)\mathscr{P}|j'\rangle]\right] \\ &= |\phi_2\rangle - (1+\mathscr{P}t)|\phi_3\rangle. \end{aligned}$$

We thus obtain $a_3 = -(1+\mathscr{P}t)$ and $b_3 = 1$. Second,

$$\begin{aligned} \mathbf{H}|\varphi_3\rangle &= |\varphi_2\rangle + \frac{1}{\sqrt{12}}[t(|23'\rangle - |24'\rangle + |26'\rangle - |27'\rangle + |29'\rangle - |30'\rangle) + \mathscr{P}t(|23\rangle - |24\rangle + |26\rangle - |27\rangle + |29\rangle - |30\rangle)] \\ &= |\varphi_2\rangle + \mathscr{P}t\frac{1}{\sqrt{12}}[(|23\rangle - |24\rangle + |26\rangle - |27\rangle + |29\rangle - |30\rangle) + \mathscr{P}(|23'\rangle - |24'\rangle + |26'\rangle - |27'\rangle + |29'\rangle - |30'\rangle)] \\ &= |\varphi_2\rangle + \mathscr{P}t|\varphi_3\rangle. \end{aligned}$$

Therefore, we have $a_3 = \mathscr{P}t$ and $b_3 = 1$.

*Present address: Department of Physics, West Virginia University, Morgantown, West Virginia 26506-6315.

[1] E. Manousakis, Phys. Rev. B **44**, 10 991 (1991); **48**, 2024(E) (1993).

[2] D. Tománek and M.A. Schluter, Phys. Rev. Lett. **67**, 2331 (1991); **56**, 1055 (1986); Phys. Rev. B **36**, 1208 (1987); D. Tománek *et al.*, *ibid.* **39**, 5361 (1989).

[3] Y. Deng and C.N. Yang, Phys. Lett. A **170**, 116 (1992).

[4] R. Friedberg, T.D. Lee, and H.C. Ren, Phys. Rev. B **46**, 14 150 (1992).

[5] J. González, F. Guinea, and M.A.H. Vozmediano, Phys. Rev. Lett. **69**, 172 (1992); Nucl. Phys. **B406**, 771 (1993); F. Guinea, J. González, and M.A.H. Vozmediano, Phys. Rev. B **47**, 16 576 (1993).

[6] S. Satpathy, Chem. Phys. Lett. **130**, 545 (1986); S. Satpathy *et al.*, Phys. Rev. B **46**, 1773 (1992).

[7] V. Elser and R.C. Haddon, Phys. Rev. A **36**, 4579 (1987); Nature **325**, 792 (1987).

[8] R. Haydock, in *Solid State Physics*, edited by H. Ehrenreich, F. Seitz, and D. Turnbull (Academic, New York, 1980), Vol. 35.

[9] J.H. Weaver, Acc. Chem. Res. **25**, 143 (1992), and references therein.

[10] D. Weaire and M.F. Thorpe, in *Computational Methods for Large Molecules and Localized States*, edited by F. Herman, A.D. McLean, and R.K. Nesbet (Plenum, New York, 1973).

[11] L.D. Landau and E.M. Lifschitz, *Statistical Physics*, 2nd ed. (Pergamon, Oxford, 1968), pp. 447–454.

[12] G. Grosso and G. Pastori Parravicini, in *Memory Function Approaches to Stochastic Problems in Condensed Matter*, edited by M.W. Evans, P. Grigolin, and G. Pastori Parravicini, Advances in Chemical Physics Vol. 62 (Wiley, New York, 1985).

[13] Y.-L. Lin and F. Nori, Phys. Rev. B **49**, 5020 (1994).